Proceedings World Geothermal Congress 2005
Antalya, Turkey, 24-29 April 2005

Clark Volcano Dredged Samples, Kermadec Trench; Mineralogy, Fluid Inclusions and Preliminary S-Isotope Characterization

Marco A. Rubio. R[1]., Patrick R. L. Browne[2] and Clemente Recio[3]

[1] Av. Universidad # 3000, Circuito de la Investigación Cientifica, Geophysics Institute, 2° Floor; 04510 - UNAM., Mexico.

marrubio@geofisica.unam.mx

2Geology Dpt., Auckland University. 23 Symonds Street, University of Auckland; 92109 – Auckland, New Zealand.

prl.browne@auckland.ac.nz

3 Dpt. of Geology and Stable Isotope laboratory, Univ. of Salamanca. Pza. de la Merced, S/N; E37008 – Salamanca. Spain.
crecio@usal.es

Keywords: Kermadec Ridge, Clark Volcano, Sr-barite, fluid inclusions, sulphur isotopes, hydrothermal.

ABSTRACT

Clark Volcano is a recently discovered volcanic edifice located on the western side of the Kermadec Ridge. It represents just one of the multiple sites where submarine hydrothermal systems occur in this region. The study of samples dredged on the margin of this volcano shows both partial replacement and direct deposition textures, as layers (up to 10 cm thick) composed of sulphates, pyrite and lesser carbonates, arranged in rithmic, thin-layered (5 to 20 mm thick) barite/anhydrite pairs. Textures and mineralogical associations may be indicative of medium-high temperature hydrothermal fluids discharged from submarine vents. Several stages were recognized. Independent layers display both chemical and $\delta^{34}S$ isotopic variations, reflecting physico-chemical changes during deposition. Analyses by XRD indicates that pure anhydrite and Sr/Pb-rich barites are the dominant mineralogical phases. Silica forms are very rare and occur only in early paragenetic stages or associated to clay minerals. XRF analyses of sulphates suggest that Sr and Pb replace Ba in the barites, while both Ba and Sr may substitute for Ca into the anhydrite structure. Anomalous Zn and Sr contents appear to be preferentially associated with barite rather than anhydrite. Liquid-rich fluid inclusions are rare, whereas vapor-rich ones are more common. Homogeneization temperatures on primary liquid-rich fluid inclusions in anhydrite vary from 210 to 215°C and ice-melting temperatures range from –8.9 to –9.3ºC. Preliminary sulphur isotopic data from individual layers indicate that sulphate minerals are depleted in the heavy isotope ($\delta^{34}S$ = 14.5 to 19.2‰) with respect to actual seawater. The largest ^{34}S depletion was found on anhydrite at the anhydrite-pyrite interphase ($\delta^{34}S$ = 5.0‰). Late crusts and rims above early hydrothermal sulphates consist of very pure anhydrite, whose isotopic signature is almost identical to contemporaneous seawater ($\delta^{34}S$ = 19.2 to 20.4‰). The hydrothermal deposits of Clark volcano differ from other systems; its dominant anhydrite/barite layered products, low silica, and elevated Sr, Ba and Zn content could be indicative of high W/R ratios due to high permeability conditioned by the rock texture and the medium-temperature leaching effect K-rich lavas.

1. INTRODUCTION

Submarine volcanism and associated hydrothermal activity has been consistently documented along the southwest East Pacific Ridge for the last 25 years (Graham et al., 1988; Rona, 1988; Rona and Scott,1993). Those studies have revealed the strong influence of seafloor hydrothermal circulation as a heat and mass exchange mechanism between the ocean and the oceanic crust (Baker et al., 1995). On the northeast offshore region of New Zealand, at least 94 submarine volcanoes occur in the Southern Kermadec Arc-Havre Backarc System (Stoffers et al., 1999a; C. de Ronde, pers. com.) which are distributed along a 2500-Km long belt (Figure # 1) spanning from White Island to Tonga. Both basaltic and andesitic submarine strato-volcanoes have been discovered since 1996. Volcanoes occur at depths ranging form 250 to 1500 m below the sea surface (Stoffers et al., 1999a; Wright et al., 2002).

Clark Volcano, on the western side of the Kermadec Ridge, is a recently discovered volcanic edifice with associated hydrothermal activity. It represents just one of the multiple submarine volcanoes with associated hydrothermal systems which are related to the Kermadec Trench. The southwestern tip of the Kermadec Ridge starts onshore North Island, New Zealand, from Tongariro and Mount Ruapehu, and also includes the Taupo Volcanic Zone (TVZ) and all the geothermal systems which occur into it. The northern offshore edge continues up to the Tonga Ridge. The subduction setting becomes more complex on both of its NE and SW ridge limits. The TVZ limits the southwestern trench, where oceanic crust of the Southwest Pacific Plate subduces underneath old continental crust of the Indian-Australian Plate. In contrast, a “crustal complex evolved into full oceanic spreading” (Stoffers et al., 1999a) characterizes the northeastern side of the trench. Clark Volcano is located just near the southern limit, where the subduction setting changes from oceanic to continental (Gamble et al., 1997).

On the northeastern offshore structural extension of the TVZ, elemental Hg, Au, Ag, As and Sb, associated with submarine hydrothermal vents, have been documented (Stoffers et al., 1999b). Recent offshore expeditions to the Central Kermadec Trench using towed cameras, seafloor dredging and also research submersible detectors have studied the submarine hydrothermal plumes discharging from volcanic craters and seafloor vents (Stoffers et al., 1999b; de Ronde, 1999a). These surveys highlight the continuity of continental hydrothermal systems into a submarine setting. Vents have been related to active normal faults (de Ronde, 1999) and both vents and craters discharge high temperature fluids (up to 370ºC).

Samples dredged on the margin of Clark Volcano exhibit textural evidence for both direct deposition of Ca-Ba sulphates and partial replacement of earlier phases. Early

anhydrite is covered by fine-grained massive anhydrite, barite and pyrite layers (each up to 10-20 µm thick). Cyclic deposition of either anhydrite- or barite-dominant phase is common. There are also some layers where even equal amounts of mixed phases coexist. No monomineralic bands were found. XRD analysis indicates that when the main phase is anhydrite, some substitution of Ca by Ba and Sr does occur, while if barite is dominant, Pb-Sr replaces for Ba. High values of Zn (up to 2200 ppm) and Sr (up to 10800 ppm) and anomalous contents of Cu (up to 300 ppm) and Pb (some 900 ppm) have been recorded by XRF analyses on selected samples.

2. ANALYTICAL METHODS

Several kilograms of dredged rock samples (recovered from a fish tracker and donated to the Geothermal Institute by Ian Smith) were first studied by hand lenses and under the binocular microscope. After detailed description of the textures, selected material was used to characterize paragenetic stages. Suitable areas, representative of each different mineralogical stage, were used to study and define the mineralogy of the hydrothermal deposit. Crystalline phases were characterized using a standard petrographic microscope. Areas appropriate for fluid inclusion measurements were identified, and homogenization/ice melting temperatures were determined using a conventional Fluid Inc. adapted U.S.G.S. heating/freezing stage to characterize the nature of the trapped hydrothermal fluid. Typically, a precission of ± 2°C for heating and ± 0.2°C for the freezing stage is commonly accomplished.

Selected mineralogical phases were studied by X-Ray Diffraction and X-Ray Fluorescence (Lewis and McConchie, 1994). Samples were fisrt hand-picked separately from each paragenetic stage, and then grinded twice for 2 minutes to < 10 µm size on a tungsten automatic mortar. Mineralogy and semiquantitative chemical composition were obtained at the Geology Dept., Auckland Univ., with the aid of µpdsm® software and XRD identification tables (MPDFDB, 1993) on the powder difractograms obtained using a Philips® XRD system at standard conditions (40 KV, 20mA, 0 to 62° 2θ scans at 0.3° steps and a speed of 0.2° per minute). $^{34}S/^{32}S$ ratios have been determined in samples obtained from seven different layers, each one carefully hand-picked and grounded to a very fine powder in an agate mortar. Stable isotope ratios were determined at the Stable Isotope Laboratory of Salamanca University. Sulphur isotopic ratios on SO_2 from sulphates (both anhydrite and $BaSO_4$) was obtained off-line, following the indications of Coleman and Moore (1978). $^{34}S/^{32}S$ ratios were determined on a dedicated dual inlet SIRA-II mass spectrometer. Replicate analyses, including chemistry, of several reference standards gave an average reproducibility of ±0,27‰ or better. Results are reported in the familiar delta per mil notation relative to CDT in Table 2.

3. GEOLOGICAL SETTING OF THE KERMADEC RIDGE

Clark Volcano is located on the southwestern edge of the Kermadec Ridge and belongs to the western Island Volcanic Back Arc, associated to the westward subduction of the Pacific Plate beneath the Indian-Australian Plate (Figure # 1). The northeasterly trending regional faulting system on the North Island of New Zealand has been interpreted as the geodinamic consequence of such subduction regime. The southwestern edge of the Kermadec Ridge includes the TVZ, which host the productive continental geothermal fields of Waireki and Rotorua. Its offshore extension to the northeast has been studied on the Whakatane Graben and the area surrounding White Volcano Island. In this area, deposits of anhydrite and silica, with anomalous concentrations of Hg, Ag, Au and Sb, are related to submarine hydrothermal activity (Stoffers et al., 1999b).

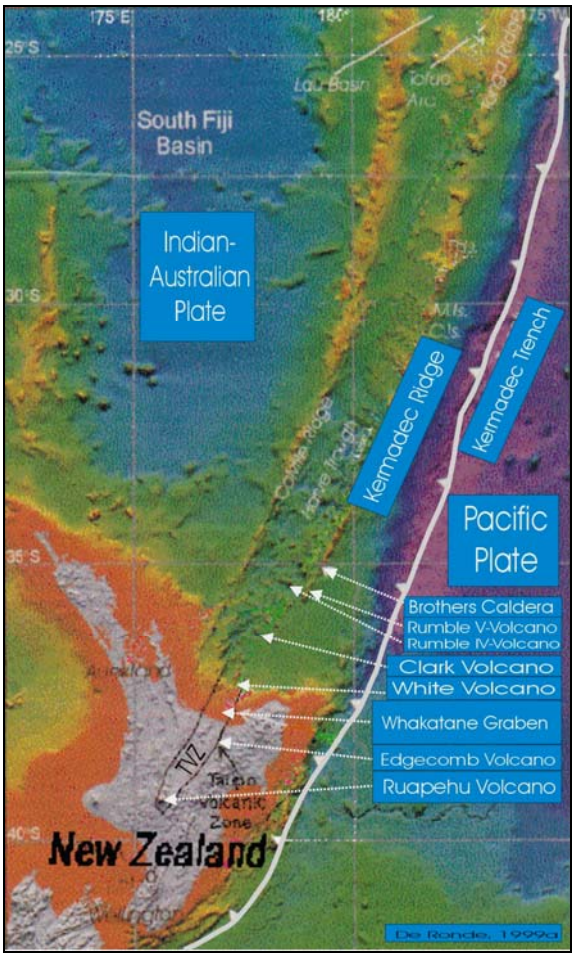

Figure # 1.- Regional tectonic setting of Kermadec Arc (modified Figure from de Ronde, 1999a).

The 1999 survey found 13 new volcanic edifices, 7 of which were defined as hydrothermally active. A new expedition was conducted to the south of the 1999 survey in April 2002, locating 11 additional submarine volcanoes (de Ronde, 2002). Recent expeditions to the western side of the Kermadec Ridge have probed the continuity of continental to oceanic hydrothermal systems into a full submarine volcanic setting, some of them also associated with regionally active normal faults (Stoffers et al., 1999b; de Ronde et al., 1999a). To date, a hundred basaltic to andesitic submarine volcanoes have been discovered between White Island Volcano and the Tonga edge (de Ronde, per. com.) revealing the continuity of the NE 30 bearing volcanic front. Southern volcanoes at the west side of the Kermadec Ridge have been constructed onto oceanic crust since the Eocene (Smith et al, 1997). This volcanic edge is composed by Edgecomb, White Island, Clark, Tangaroa and Rumble III, while Rumble II, V, Healey and Brothers Volcano belong to the central ridge (Figure # 1).

Almost all of the volcanoes in this area display similar topographic characteristics: high relief, a caldera and simple conical morphology. Brothers Volcano, however, has a larger caldera (3 km diameter) which host localized vent

fields that expell high temperature mineralizing fluids (de Ronde, 1999a). Rumble III volcano, 250 Km northeast of Clark Volcano, is formed by two constructional cones and a 600 m diameter caldera (Wright et al., 2002). Clark Volcano, which is the southernmost basaltic to andesitic submarine strato-volcano occurring along the west side of the Southern Kermadec Ridge, exhibits an even simpler morphology, consisting of two high constructional cones, without associated caldera (Wright et al., 2002; de Ronde, 1999). It was originaly defined as hydrothermally inactive, although present data allow its consideration as latent, rather than inactive.

The geochemistry of Kermadec lavas has been studied in detail by Smith et al. (1997). These authors define the nature of volcanic activity and correlate it with the tectonic setting. Low-K series with bimodal silica contents, are the typical volcanic products from the Kermadec Volcanic Arc. However, older basaltic and basaltic-andesitic lavas contrast with younger dacitic and rhyolitic lavas (Smith et al., 1997, Figure # 2).

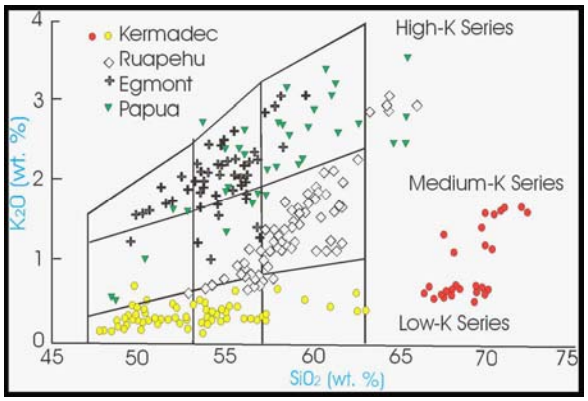

Figure # 2.- K_2O vs. SiO_2 plot of different Arc-Type lavas. The Kermadec volcanoes belong to the low-K series, and display bimodal silica concentration (from Smith et al., 1997).

4. CLARK VOLCANO GEOLOGY

Clark Volcano belongs to the southwestern volcanic front of the Kermadec Ridge and is located just 50 Km west of the Kermadec Trench. It is constructed onto oceanic crust and represents the transition from the oceanic to the continental arc. In contrast, White Island Volcano, just 200 Km to the SW, is constructed onto continental crust. Three types of lavas make up Clark Volcano's edifice. These are the typical older basaltic and basaltic-andesite Kermadec lavas, which are characterized by both low-K and low-Mg volcanic products (Gamble et al., 1997; Smith et al., 1997). In contrast, recently found K-rich lavas from Clark Volcano (Figure # 3) are composed of olivine (Fo_{89}-Fo_{80}); chromian spinel, and phenocrysts of Mg-rich clinopyroxene. The plagioclase, mostly as groundmass, is An_{78}, and its silica content is nearly constant at 50% (Gamble et al., 1997). High Ba (600 ppm), Rb (46-60 ppm) and Cs (1ppm) characterize these K-rich magmas. This unexpected petro-geochemical pattern of K-rich lavas has been interpreted by Gamble et al. (1997) as a one of the most primitive magmas on the Kermadec Arc, although they conclude that "even these melts must have experienced some modification by crystal fractionation". There are also younger rhyo-dacitic and dacitic lava flows produced during recent effusive events, which are apparently more common in the northern Kermadec Arc.

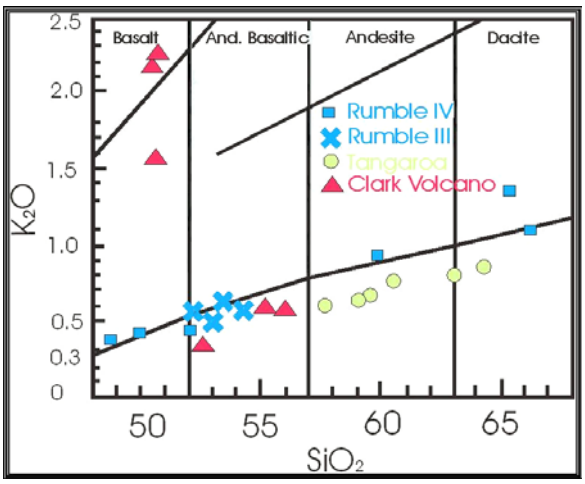

Figure # 3. – K_2O vs. SiO_2 diagram. The samples from Clark Volcano are compared with data from Rumble III, IV and V and Tangaroa Volcanoes in the southern Kermadec Arc. (Figure from Gamble et al., 1997).

A recent towed-camera investigation on the crest and flanks of Clark Volcano zone indicates that two styles of eruptions control its morphology. The distribution and type of lava flows and pyroclastic deposits have been interpreted as transitional between effusive and explosive events (Wright et al., 2002) and reflects the dynamic behavior of submarine volcanism. Below 700 m water depth massive/blocky flows, pillow lavas, pillow and angular block talus and granule-sand volcaniclastics detritus (5-20% substrate mode) are common. Above 450 m depth water level, sand lapilli (50-100% substrate mode), massive flows, pillow lavas and coarse talus are the dominant textures. Between 600 to 700 meters water depth, a mixed substrate of sand lapilli and massive blocky flows marks the boundary of those two types of volcanic emissions. Phreatic and phreatomagmatic eruptions occur at 670 to 860 meters water depth. Those effusive materials, under 860 meters of seawater column pressure, spread laterally and cover the margins of the volcano. Fallout material forms a non-consolidated lid that favours liquid and gaseous hydrothermal venting. Hydrothermal alteration of basaltic lavas, basaltic-andesites and recent dacites appears to be more common on the northern cone of Clark Volcano (Wright et al., 2002).

5. RESULTS

5.1 Mineralogy of Clark Volcano dredged samples

For practical purposes, the paragenetic description of samples emphasized textural relationships. All Clark Volcano dredged samples consist mainly of sulphates, with minor sulphides. No fragments of the volcanic host rock were found. The most common product of the hydrothermal activity are anhydrite mounds, barite and Sr-rich barite. Pyrite is found either as massive agregates (up to 1 cm thick, composed by hundreds of tiny cubic crystals) or else finely dispersed in late events. Successive stages, grouped on the basis of similar crystal size, texture and relative position, were grouped into four correlative events, termed I to IV below. Stage I represents early events, which display few variations on textural characteristics and crystal size. It usually comprises some 80% of the main groundmass of the whole sample. Stage II is related to intermediate banding phases and is commonly represented by euhedral species of both barite or anhydrite associated with pyrite. Finally,

stages III and IV represent late events related with direct deposition of sulphates and halite sediments from the seawater column or associated with poorly developed organic activity. The last alteration processes of early stages produce clays which may be responsible for the Al, K and silica contents determined by XRF.

5.1.1 Stage I

Early stages are composed mainly by massive white and very fine-grained euhedral sulphates. These materials form almost all the groundmass (up to 75%) of the samples. Bands of bladed subhedral crystals (up to 10 μm size) and prismatic aggregates (micrograph # 1) are close enough to construct a semi-hard, dense matrix, which supports later stages (Figure # 4A and B). Petrography and X-ray diffraction data indicate that it is composed mostly of pure anhydrite and both minor Sr-Pb/Ba-sulphate $(Sr,Ba)SO_4$ and $(Sr,Ca)SO_4$. Barium accounts up to 22.1% wt., and Ca 17% wt.

On some areas, earlier rhombic crystals of pure anhydrite are broken and cemented or partially replaced by a second phase of microcrystalline anhydrite mixed with clays. Jigsaw texture on those brecciated events is poorly developed. Additionally there are some rims of very fine and soft botryoidal pyrite, with lesser ammounts of calcite and chlorite surrounding earlier angular anhydrite fragments. Pyrite was documented only in samples that were very fine-grained, frecuently as ≈ 5 μm thick layers composed of fine anahedral crystals. This association also occurs as 0.5 mm thick layers after individual bands of microcrystalline anhydrite. On some areas, partial replacement of green-colored, early, euhedral anhydrite by granular anhydrite-calcite is the dominant textural feature. Calcite is just a minor phase associated to sulphates. Barite is the second most frequent mineral found on samples dredged from Clark Volcano and on Stage I, it is usually found finely mixed with anhydrite. Early stage barite is very fine-grained (5 to 10 μm size) and forms granular aggregates with earthy texture, but varies to subhedral barite. No replacement of barite by carbonates was observed. Silica was recognized in the groundmass and represents only a minor fraction of stage I (accounting for less than 0.30%). This value is in agreement with both petrographic and XRD data, where silica is almost absent and might be related to clay alteration products. Trace quantities of Hg and Ag/Pb/Sb-sulphate exist as an additional component. Whole rock analyses (table # 1) from less altered samples of fine-grained stages I and IIa shows a negative relationship between Ba (barite) and Ca (anhydrite) indicating the dominant cation bound. Both cations account mainly for sulphate phases (>95%). Total iron (Fe^{2+}, Fe^{3+}) can reach up to 1.3%, and Sr up to 6700 ppm. High contents of base metals (2200 ppm Zn and 700 ppm Pb), associated with early stage hydrothermal deposits, have been also recorded.

5.1.2 Stage II

This stage has been further divided into two sub-stages, according to their mineralogy and texture.

Stage IIa refers to a perfectly euhedral, bladed anhydrite (3 to 6 mm length size), that forms in open spaces or cavities located into the groundmass. Crosscutting textural relationships between stages I and II occur only before banding, and even then it is not a common feature. Perfect radiating and semitransparent prismatic crystals of anhydrite also grow from previous events, and are indicative of a more favorable environment of formation (Figures # 5A and B). Wherever there are open spaces, the growth of larger, parallel and prismatic, euhedral crystals, are more common. X-ray Diffraction on bladed euhedral crystals from stage IIa highlights the abundance of anhydrite. This result is in agreement with X-ray fluorescence analysis, consistent with pure calcium sulphate (up to 96%). Stage IIa may also be represented by white bands (up to 10 mm thick) of tabular and transparent, barren, anhydrite (10-30 μm length), and also minor, radiating, yellow-colored barite (10 to 15 μm length). The stage IIa displays the lowest concentrations of total Fe, Ba, Al, Sr and Si respect to total rock analyses and other phases. Those bands alternate successively with thinner and darker bands of stage IIb. Differences on both color and crystal size are indicative of the dominant sulphate species.

Sub-stage IIb represents a continuous and repetitive thin banding of fine-grained tabular barite and anhydrite. White bands (20 μm thick) are dominated by barren anhydrite and separated by darker bands (5 to 10 μm thick) composed by barite-pyrite plus organic matter. Bulk composition of overall Stage IIb reveals that the dominant phase is euhedral anhydrite, in good agreement with petrographic studies. Such thin sheet-like sulphates have developed weak syn-sedimentary plastic deformation textures, that indicate movement of the unconsolidated deposits over the seafloor (Figures # 5A and B). General texture of dark bands is in the form of compact aggregates and randomly-distributed perfect tabular crystals of barite (5 μm large), finely mixed with disseminated subhedral pyrite and lesser anhydrite. In contrast to other events, XRD analysis of carefully selected material from darker layers (table # 1) indicate that these are made up mainly of Ba/Sr-sulphate, which is always present in association with high concentrations of subhedral pyrite (up to 40% and 5 μm size).The highest Ba and Sr concentrations were recorded on this stage. XRD analyses also point out some degree of cationic substitution of Ba by Pb in barite crystals. X-ray fluorescence results support the above (Figure # 6). Ca-carbonate and Mn oxide are present only as a small fraction of the sample. High “d”-spacing values recorded by XRD for these samples correspond to a zeolite L, but further research should be required to properly define its nature.

Detailed separation of additional pink-brown-colored bands from stage IIb, just after the matrix, was also possible, and XRD analysis hold that its chemical composition is represented by Ba/Pb-sulphate $(Ba,Pb)SO_4$ mixed with less pure anhydrite. Neither celestite nor hokutolite were identified by petrographic analysis; however X-ray diffraction and fluorescence results indicate that cationic substitution on the barites occurs also on this pink layer. Ca presence can be explained by a small contamination by anhydrite crystals during separation, or because of partial substitution of Ba by Ca. Total Fe of overall stage IIb accounts for up to 17800 ppm due to the presence of finely disseminated pyrite (table # 1). High concentrations of Na and Cl on samples Stage IIb and IV are related to some marine halite crystals (2 μm size) contamination during the separation procedure.

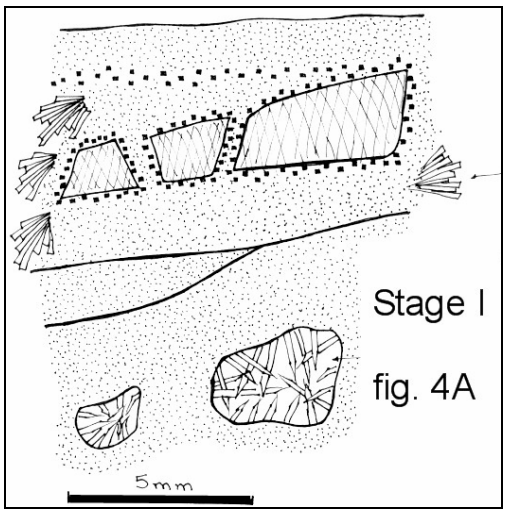

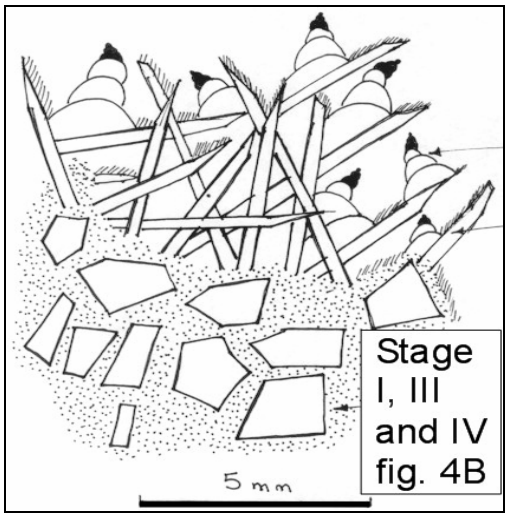

Figure # 4. A) Stage I groundmass, composed by microcrystalline anhydrite-calcite-chlorite, cements earlier fragments of euhedral anhydrite with jigsaw texture. Fine-grained botryoidal pyrite with calcite surrounds those fragments. Stage III, showing the open spaces filled by bladed anhydrite with a cover of thin iron oxides and a Hg phase; B). Stage I, at the base of the sample, is composed by massive Ba/Pb-sulphate, mixed with microcrystalline anhydrite that cemented fragments of earlier anhydrite. Stage III bladed anhydrite with a thin cover of yellow sulphur. Stage IV botryoidal Ba/Sr-sulphate, with botryoidal fine-grained aggregates of pyrite.

5.1.3 Stage III

This stage can be observed covering stages I or II, or also developed from cavities and open space. It consists on perfect crystals of bladed and prismatic anhydrite and lesser barite (2 to 4 mm size). Larger, transparent and euhedral crystals, up to 4 mm size are quite common. Cavities near earlier stages contain also prismatic blades of this anhydrite with Fe-oxide rims, and small subhedral crystals of phyrrotite and an unidentified Hg-phase. Where pores are bigger at sites near surfaces of stage II, larger crystals can be seen, but in that case the dominant sulphate species is radiating barite. Such individual crystals are elongated, up to 8 mm length. If rhombic crystals of anhydrite are present then there is always some gypsum associated, as well as calcite and fine-grained botryoidal pyrite (Figures # 4 A and B). Total Fe concentrations can reach up to 19200 ppm, closely matching the distribution of pyrrhotite and pyrite on this stage. An important point is that these samples display the higher Si, Ca and Al concentrations, perhaps due to the presence of some clay and zeolite crystals remaining during the separation processes. Mg can be as high as 2800 ppm; the highest concentration found on Clark Volcano samples. Base metals are also present, with up to 900 ppm Pb or up to 1200 ppm Zn (table # 1).

Element %	Stage I	Stage IIa	Stage IIb	Stage III	Stage IV
Si	0.27	0.16	0.28	0.43	0.41
Ti	0.03	0.03	0.05	0.02	0.02
Al	0.22	0.09	0.21	0.26	0.25
Na	0.67	0.69	8.93	1.99	1.7
K	0.06	0.05	0.06	0.15	0.15
Cl	1.51	1.05	10.4	3.13	3.13
Cu	0.02	0.01	0.02	0.03	0.03
Pb	0.07	0.04	0.06	0.09	0.09
Sr	0.67	0.25	1.08	0.026	0.026
V	0.02	0.02	0.05	0.01	0.01
Zn	0.22	0.8	0.15	0.12	0.11
Zr	0.04	0.02	0.03	0.03	0.03
Ba	22.1	3.15	35.5	4.38	4.29
Ca	16.8	29.8	4.2	31.7	30.64
S	27.7	29.3	20.9	30.3	30.1
O	30.7	37	19	36.4	37.8

Table # 1. X-Ray Fluorescene analyses of Clark Volcano samples.

5.1.4 Stage IV

Botryoidal textures are the most common feature of this stage. Late anhydrite phases occur as a soft, milky and semitransparent snow-flake-like accumulations on top of stage III bladed barite and gypsum (Figure # 4B). Radiating, euhedral, pure anhydrite crystals also grow from any of the earlier stages.

Samples from stage IV were recovered by meticulous separation of globular concretions (2 to 4 mm diameter) on the top of euhedral gypsum crystals, and were also characterized by XRD. Rims of this material are crowned by very fine-grained botryoidal pyrite (up to 10 µm diameter), and a thin rim of sulphur. Associated to this texture is the presence of elongated and very thin filaments, tubular multi-cylindrical organisms, and small convoluted-globular soft-shells. Worm-like holes on the matrix are present and very tiny filaments are preserved around the organic cavities. Similar filaments have been found on other submarine hydrothermal systems (e. g. vents on Galapagos Rift, Holger, 1983; de Ronde et al., 1999b).

On some samples, late calcite/aragonite mammillae, or coral-like textures, commonly cover the surface of any of the earlier stages. These late materials are milky, very soft and semi-opaque and display growth rings at microscopic scale; perhaps the result of organic activity. XRD profiles acount for the clay mineralogical species present in the last deposition and alteration process. Ba/Pb-sulphate is present in lesser quantities, but in contrast, pure anhydrite plus cerussite ($PbCO_3$) are the most important phases. Halite crystals were not identified by petrographic analyses, but XRF analyses reveal it is present by as much as 5%. Stage IV samples also contain “pinacoidal” gypsum, but only as the latest deposit after anhydrite, or else filling cavities.

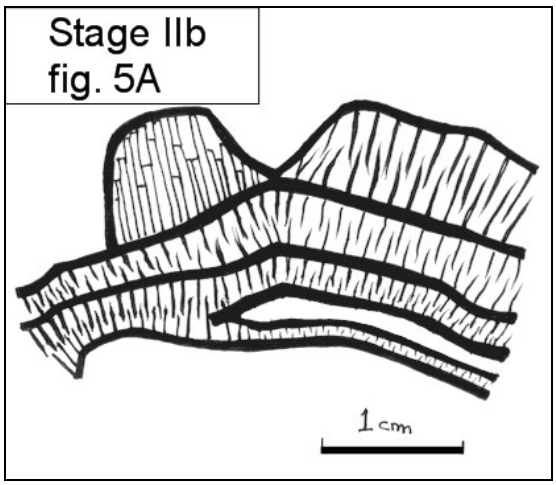

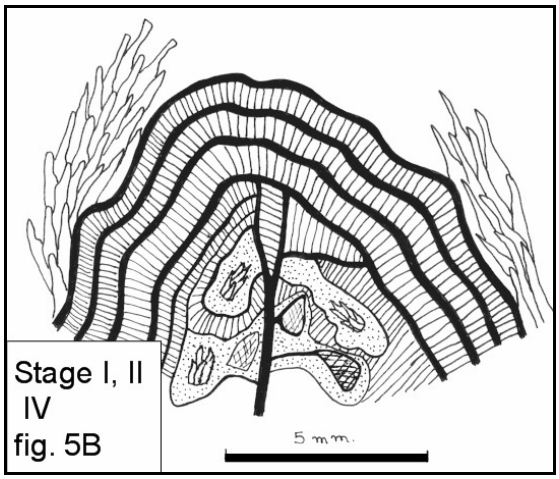

Figure # 5. A) Fine banding texture of Stage IIb (up to 1-cm thick). White prismatic and euhedral anhydrite crystals and dark layers of strontium barite-pyrite up to 3 mm thick displaying weak deformation pattern; B) Fragments of barren early anhydrite (Stage I) with partial replacement by fine-grained anhydrite-barite-pyrite. Continuous banding of white euhedral anhydrite (stage IIa) inter-bedded with dark layers (stage IIb) composed of fine barite-pyrite-anhydrite aggregates. Stage IV composed by coral like texture of milky calcite/aragonite growths.

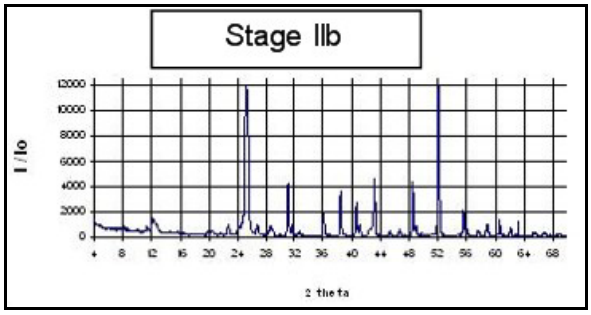

Figure # 6.- X-ray diffraction profile for Stage IIb of Clark Volcano dredged samples. (2θ from 0 to 70 degrees).

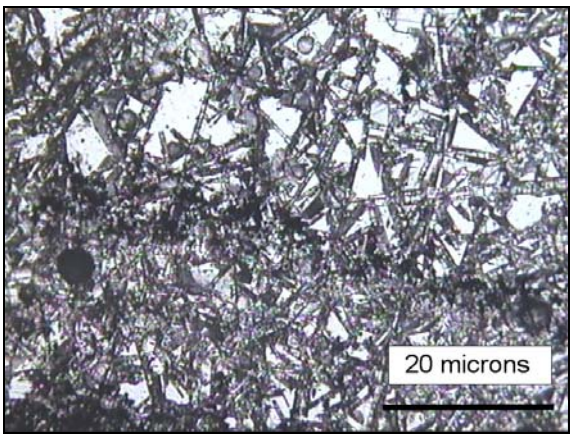

Micrograph # 1. Fine-grained, tabular-shaped anhydrite crystals of Stage I. This material constitutes the matrix of Clark Volcano dredged samples [20X, NL, TL].

Micrograph # 2. General texture of Stage IIb. Cyclic barite-pyrite/anhydrite layers show syngenetic deformation. Dark bands are composed of finely diseminated euhedral crystals of pyrite plus barite. Light layers are an anhydrite-dominated phase [2.5X, NL, TL].

5.2 Geothermometry

Homogenization temperatures were measured only in anhydrite crystals because of the lack of suitable fluid inclusions on barite and calcite. The petrography of the fluid inclusions on anhydrite highlights its primary origin, following the empirical criteria given by Roedder (1984) and Goldstein and Reynolds (1994). Even when these inclusions are not common, when they do occur, however, are in the form of the two-phase, liquid-rich type, and show

quite consistent liquid/vapor ratios (micrographs # 3 and 4). Vapor-rich fluid inclusions are slightly more abundant and larger. Both types of inclusions are parallel to facets of individual crystals, display similar size, and are present as tubular or rectangular shaped groups. Additionally, a dark orange fluid near vapor-rich fluid inclusions hosted in anhydrite was observed.

Homogeneization temperatures (8 measurements) were made on Stage II anhydrite crystals associated to pyrite. Primary liquid-rich fluid inclusions (5-10 μm) homogenized consistently at 210 to 215°C. Those results agree with the consistent liquid/vapor ratios and migth be considered as the minimum temperature of formation in absence of immiscibility proof.

During heating, critical temperature measurements (n=4) made on vapor-rich fluid inclusions gave values of -86.6 ^{o}C. Those temperatures were defined by a sudden jerk inside the inclusion and a nearly undistinguished change in coloration, indicating a methane compound being hosted by the inclusions. If methane is almost a pure phase inside the inclusions, homogenization temperatures range from -97 ^{o}C to -82 ^{o}C (Goldstein and Reynolds, 1994). The critical point for pure methane is -82.1 ^{o}C at 46.3 bars.

Eutectic temperatures on liquid-rich fluid inclusions from Clark Volcano samples give values of -44.2 ^{o}C to -33.7 ^{o}C (2 measurements), however there is a possible variation of ± 3^{o}C on each measurement. Eutectic temperatures for the systems defined give a good approach to the type of brine being studied. The determination of eutectic temperature of the system was used to known what kind of brine is trapped in anhydrite crystals. Goldstein and Reynolds (1994) provide predicted, predicted metastable, and observed eutectic temperatures for NaCl-$CaCl_2$-H_20 system; those temperatures are -52 ^{o}C, -70 ^{o}C and –47 to -53 ^{o}C respectively, representing a eutectic composition of -1.8% NaCl and 29.4% $CaCl_2$. Measured eutectic temperatures may indicate a complex mix of aqueous ions inside the inclusion, considering a seawater-dominated system and the abundant anhydrite deposited.

Measured melting temperatures of last ice trapped in liquid-rich fluid inclusions from anhydrites varies from –8.2^{o}C to –9.6^{o}C (4 measurements); in contrast the ice-melting temperature of seawater is –1.9°C. Aqueous sedimentary environments are very complex. The concentration of ion species influences not only the stability of the host mineral but also methane solubility. Seawater contains mainly Na^{+}, K^{+}, Ca^{2+}, Cl^{-} and $SO_4^{=}$ as dominant ions (Goldstein and Reynolds, 1994). If a hot hydrothermal fluid laden with Zn^{+}, and Ca^{2+}, Sr^{+} and Pb^{2+} were to mix with seawater, the relative salinity of the resultant fluid should gradually increase.

6. δ^{34}S-ISOTOPIC SIGNATURES

Sulphur stable isotope ratios have been determined on the different layers described above on Clark Volcano dredged samples (table # 2). Average whole-rock δ^{34}S measured is 16.2‰. Preliminary results on individual layers show a variation of δ^{34}S from 5.0 to 19.2‰, indicating that sulphate minerals are slight to moderately depleted with respect to actual seawater (δ^{34}S = 20.4‰). Early stages are 2.6 to 5.6 ‰ lower with respect to present-day seawater sulphate. The larger variation observed corresponds to stage IIb anhydrites ($\Delta^{34}S_{SW\text{-}Anh}$ = 5.0‰). These sulphates grow just above 1 cm thick massive, fine-grained pyrite. In contrast, stage IV late crusts and rims cover early hydrothermal sulphates, and are composed by nearly pure anhydrite, whose isotopic signature (δ^{34}S = 19.5‰) reveals that it is almost equal to contemporaneous seawater isotopic composition. These variations from isotopically heavy to light sulphates are also related to the dominant mineralogy of each band. Barite crystals show the smallest difference, but anhydrite reflects a wider espectrum of isotopic compositions.

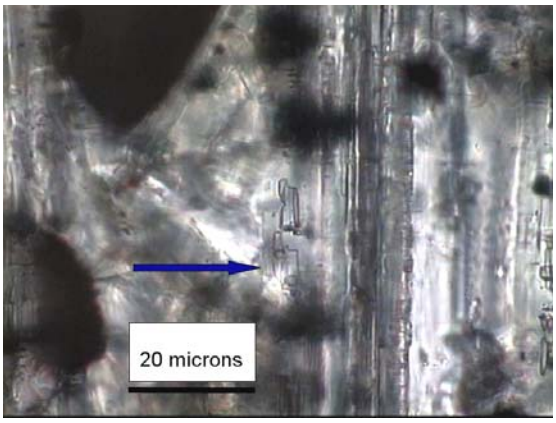

Micrograph # 3.- Anhydrite crystal hosting primary, liquid-rich fluid inclusions. Darker areas correspond to associated crystals of pyrite.

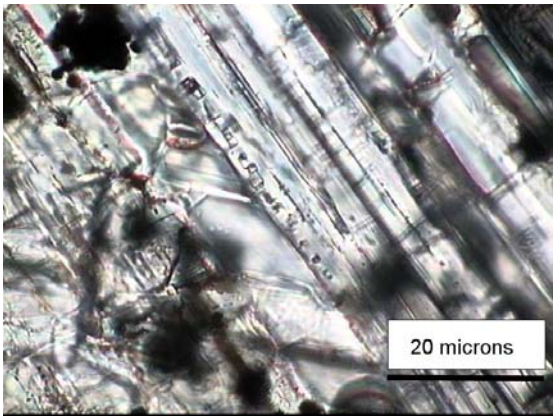

Micrograph # 4.- Euhedral and tabular anhydrite crystal hosting liquid-rich primary fluid inclusions. Darker areas correspond to crystals of fine-grained pyrite associated with anhydrite and barite.

7. DISCUSSION OF CLARK VOLCANO SAMPLES RELATED TO SUBMARINE HYDROTHERMAL VENTS

Enrichment of major and trace elements on hot springs from continental geothermal systems is a commonly observed process. High and medium-temperature fumaroles related to igneous activity (Scott, 1997) at the margin of the volcanoes is also an operative albeith intermitent phenomena. Submarine hydrothermal systems provide large quantities of chemical elements like K, Ba, Zn, As, Pb, Au, Ag (Bloch and Bischoff, 1979 ; Fouquet et al., 1991; Scott, 1997) and Hg, Mn and S to the ocean (de Ronde, 1999; 1999b) and supply an excess hydrogen sulphide which favours organic activity under anaerobic and reducing conditions. Many studies have found relevant similitudes between actual submarine hydrothermal systems and antique masive sulphide deposits. On the later, sulphur is present into the molecular structure of several sulphide and

sulphate phases. The most common mineral found on this type of deposits is pyrite (FeS_2), although monosulphides, sulphosalts and sulphates are all but uncommon. Even among pyrite crystals, several formation stages responding to contrasting processes, have been reported. Moreover, sulphur can be present as acid volatile sulphides, elemental sulphur and as a organic sulphur (Canfield et al., 1986) in marine sediments and ahales.

Stage	Mineral Phase (dominant)	$\delta^{34}S$
I	Anhydrite (Clk 4a*)	17.8
I	Anhydrite (Clk 5b)	14.5
IIb	Anhydrite (Clk 3)	5.0
III	Barite (Clk 4c)	17.9
III	Anhydrite (Clk 5a)	20.4
III	Anhydrite (Clk 8)	16.8
IV	Barite (Clk 9)	19.2
IV	Anhydrite (Clk 7)	19.5

*Table # 2.- Sulphur Isotope analyses of Clark Volcano´s dredged samples. All data are ‰ relative to CDT (*average of 3 measurements).*

Recent expeditions to the Whakatane Graben, the NE offshore extension of the TVZ, reported the presence of elemental Hg plus extensive deposits of sulphur at the bottom of the seafloor (Stoffers et al., 1999b; de Ronde, 1999a). These acumulations, typically characterized by mounds of anhydrite surrounded by silica, are the product of hydrothermal venting related to active regional faults; bedded sulphur deposits are also common (Stoffers et al., 1999b). The fluids released by the vents were laden with high contents of Au, Ag, As, Sb and Hg. Submarine hot springs at depths between 160 and 200 meters vented CO_2 gas at temperatures from 180 ^oC to 200 ^oC (Stoffers et al., 1999b; de Ronde, 1999a). On 1999, the Tangarora research ship discovered the emission of hydrothermal plumes associated with submarine volcanism on the northeast side of Clark Volcano. This survey revealed high temperature fluids escaping from vents and volcanic craters. Fluids analyzed were laden with high concentrations of base and precious metals (up to 18% Zn, 15 % Cu and 6 ppm Au; de Ronde, 1999a). Density and temperature differences between the sub-saturated medium and the hydrothermal fluid allowed the hydrothermal plume to move away from the vent site, before temperature changes modified concentration to saturation conditions, precipitating sulphides. In some favorable cases this resulted in the accumulation of economic deposits (Scott, 2001).

The discovery of Brothers Caldera, on the northeast part of the Kermadec Ridge (Figure # 1) opened to research one of the most important areas where sulphide mineralization has been related to high temperature submarine hydrothermal systems. Rising plumes are gradually diluted by seawater, but those mixed plumes can move and expand tens to hundreds of meters above the vent site, and move laterally as a distinct layer (de Ronde, 1999a; Baker et al., 1995). In the Brothers Caldera area, the reported mineralogy of the hydrothermally altered rocks and chimneys surrounding “black smokers” includes an association of pyrite-anhydrite-sphalerite plus Fe-oxides and silica crusts (de Ronde, 1999).

Recent investigations catalogued Clark Volcano as inactive, both respect to volcanic emissions and hydrothermal activity. Dredged samples, however, display both similarities and differences with respect to Tangarora and Whakatane hydrothermal deposits. Mound-like layered deposits of Ca and Ba-sulphates; 215°C homogenization temperatures from primary liquid-rich fluid inlusions in anhydrite; anomalous concentrations of Sr, Zn, Pb and Ag on the samples examined, plus $\delta^{34}S$ isotopic results, all might account for past submarine hydrothermal activity on the margins of Clark Volcano.

However, marked differences should be noted regarding the physico-chemistry of mineralogical species found on Clark Volcano samples. At Calypso site, anhydrite mounds were reported, but they occur at <200 m water depth, <200°C temperature and usually are associated mainly to silica, native sulphur and Hg, Sb and As (de Ronde, 1999a). In contrast, the present study documents minimum amounts of silica and calcium carbonates, that if at all present, occur just in early Stage I and late Stage IV. Neither Fe-oxyhydroxides or manganese-oxide phases were identified. The dominant phase is anhydrite rather than barite, and sulphates are notably enriched in Ba and Sr.

The barite group of minerals is formed by the fundamental structural anion SO_4^{2-} and one of the large divalent cations Ba, Sr or Pb. The degree of cationic substitution in anhydrites and barites is limited by the coordination number of oxygen (Hanor, 1973) and especially by electric charge and size of the divalent cation to be substituted. Heinrich (1965) studied the substitution behaviour on some ore suites, although no in-depth treatment was reported. In Clark Volcano anhydrites, Ca appears to be partly replaced by Sr and Ba while substitution of Ba by Pb or Sr appears to be a common process. XRD traces did not detect pure anglesite, and just one sample displayed some of the celestite peaks. XRF analysis, however, shows that Sr is present in sulphates, varying from 260 ppm on late stages III and IV up to 10800 ppm on selected material from stage IIb related to pyrite agregates. Due to its retrograde solubility, anhydrite and barite precipitate from cooling hydrothermal fluids. Experimental studies show that anhydrite forms when sulphate-bearing fluids circulate through the host rock, or by evaporation of seawater above 42^oC (Deer et al., 1978). At lower temperatures, the salinity of the brine should be higher to produce the deposition of anhydrite. Otherwise, at lower salinity, apparently gypsum should form. Experimental data also indicate that barite should precipitate at higher temperatures, given its low solubility in water; however, those experiments also indicate that barite solubility increases in presence of chloride species (Deer et al., 1978). In submarine hydrothermal systems, reduced, saline fluids, transport Ba, which on interaction with cool seawater, precipitates as barite (Thompson and Thompson, 1996). Small pyrrhotite crystals associated with early massive anhydrite of Clark Volcano dredged samples indicate reducing conditions. On the Broadlands-Ohaaki continental geothermal system, pyrrhotite indicates poorly permeable zones under reducing conditions, and its formation has been related to separated

steam trapped by impermeable layers (Ellis and Mahon, 1977).

Stable isotopic analysis on geological samples has been used as a tracer for geochemical processes (Hoefs, 1997) and may reflect the physico-chemical pathway of hydrothermal solutions. The $\delta^{34}S$ of contemporaneous seawater has been estimated at 20.4‰; however as it is also the case for $\delta^{18}O$, it could be controled by several geological processes. Both low and high temperature alteration of Mid Ocean Ridge Basalts; pervasive water rock interaction; input of meteoric elements as rivers or storm precipitation above sea level … all contribute to keep more or less fixed this reference value (Hoefs, 1997). All the $\delta^{34}S$ values of barites and anhydrites from Clark Volcano are lighter than seawater sulphate. On barite-silica chimneys from the Sumisu Rift, the $\delta^{34}S$ value from Ba-sulphates are slightly higher than seawater (21.7 to 22.3‰), and this has been interpreted as an excess contribution of seawater sulphate to the precipitation of hydrothermal barites (Urabe and Kusakabe, 1990). Early and intermediate anhydrites from Clark Volcano are moderately depleted with respect to seawater sulphate. Where pyrite is the dominant phase, the anhydrite displays the largest $\delta^{34}S$ deviation. Late phases show only slight deviation of $\delta^{34}S$ respect to seawater. The kinetics of sulphur isotopic exchange reactions in solutions have been studied by Ohmoto and Lasaga, (1982), that demonstrated that the fractionation factor for aqueous S-bearing mixtures are both temperature and pH strongly dependent (Hoefs, 1997). Moreover, isotopic equilibrium below 350°C cannot be attained during coprecipitation of sulphate and sulphide minerals (Ohmoto and Lasaga, 1982). The low $\delta^{34}S$ values of early sulphates may result from mixing of a dominantly hydrothermal fluid with seawater sulphate near the vent site. Homogeneization temperatures from 210 to 215°C, and high salinities, may be related to nearby exhalative centers, where a primary mantelic sulphur source mixed with seawater sulphate. High values of Sr and Pb in anhydrite and barite layers may be the result of intense leaching of the upper crust of K-rich basalt by the hydrothermal fluid circulating through the high primary porosity of the upper 450 m of substrate below the sea surface floor. The inhomogeneous $\delta^{34}S$ values documented on sulphates from Clark Volcano indicate cyclically changing hydrothermal fluid / seawater ratios. $\delta^{34}S$ values slightly lower than seawater sulphate characteristic of stages I, III and IV suggests that even when primary sulphur from the host-rock is an important component, seawater-derived sulphate is dominant in the mixture. Perfect anhydrite crystals, grown in open spaces, and associated to gypsum, have $\delta^{34}S$ values equal to contemporaneous seawater, suggesting that hydrothermal activity ceased somehow at an early stage.

8. CONCLUSIONS

Clark Volcano dredged samples show textural characteristics similar to some exhalative deposits. Mound-like deposits are composed by layered Ba-Ca sulphate products, pyrite and some clays. These characteristics may allow considering the submarine hydrothermal system of Clark volcano as presently dormant. Sulphate products reflect past activity.

Homogeneization temperatures (210-215°C) and high salinities may be related to mixing of the hydrothermal fluid with seawater near the vent site. The presence of pyrrhotite associated to sulphates, plus fluid inclusions filled with methane, are indicative of reducing conditions of precipitation.

Hydrothermal deposits of Clark volcano differ from other submarine hydrothermal systems. They are composed almost entirely by layered sulphate products. High Sr, Ba and Zn content on sulphates are related to leaching, at hydrothermal temperatures, of the basaltic host rock, considering moderate primary porosity.

Cyclically changing seawater / hydrothermal fluid rates near the vent site are directly related to variations on both the dominant Ca-Ba sulphate and the $\delta^{34}S$ isotopic value acquired. Low $\delta^{34}S$ isotopic values are related to primary sulfur sourced from the mantle, while higher values are seawater-sulphate controled, but still with a moderate contribution from the hydrothermal fluid. Isotopic equilibrium seldom can be reached on those complex conditions.

9. ACKNOWLEDGEMENTS

This research was originally supported as part of a Diploma Project by the Geothermal Institute, Auckland University. Isotopic data were obtained at SGAIE, Salamanca University, as a part of student exchange agreement with UNAM. The senior author deeply thanks the knowledgeable assistance of Pat Browne and Felix Garcia. Invaluable dredged samples were kindly donated to the Geothermal Institute by Ian Smith. Thanks to Carolina R. for her support and patient wait.

REFERENCES

Baker, E. T., German, C. R. and Elderfield, H.: Hydrothermal Plumes Over Spreading-Center Axis; Global Distributions and Geological Inferences, Seafloor Hydrothermal Systems: *Physical, Chemical, Biological, and Geological Interactions*. Geoph. Mon. 91, 47-71, (1995).

Bloch S., and Bischoff, J. L.: The effect of low-temperature alteration of basalt on the oceanic budget of potassium. *Geology*, V. 7, 193-196, (1979).

Coleman, M. L. and Moore, M. P.: Direct reduction of sulphates to sulphur dioxide for isotopic analysis. *Anal. Chem*., 50, 11, 1594-1595, (1978).

Canfield, D. E., Raiswell, R., Westrich, J., Reaves, C. and Berner, R. A.: The Use of Chromium Reduction in the Analysis of Reduced Inorganic Sulfur in Sediments and Shales. *Chem. Geol*., 54, 149-155, (1986).

Deer, W. A, Howie, R. A. and Zussman, J.: An introduction to rock forming minerals, Longman. London, 462-475, (1978).

de Ronde C.: Offshore hydrothermal and mineral investigations. Globe. *Institute of Geological and Nuclear Sciences Newsletter*. Vol. 12, July. 8-9, (1999a).

de Ronde C. and Ebbesen, T. W.: 3.2 b y of organic compound formation near seafloor hot springs. *Geology*, Sept., Vol. 24, No. 9, p. 791-794, (1996b).

de Ronde C.: Researchers hunt for rare seafloor hot springs. *Globe*, GNS, media releases, (2002).

Ellis A. J. and Mahon, W. A. J.: Chemistry and Geothermal Systems. Energy Science and Engineering Resources, Technology, *Management. Academic Press*, New York, (1977).

Fouquet, Y., Von Stakelberg, U., Charlou, J. L., Donval, J. P., Erzinger, J., Foucher, J. P., Herzig, P., Mühe, R., Soakai, S. M. W. and Whitechurch, H.: Hydrothermal activity and metallogenesis in the Lau Basin. *Nature*, 349, 778-781, (1991).

Gamble, J. A., Christie, R. H. K., Wright I. C. and Wysoczanski, R. J.: Primitive K-Rich magmas from Clark Volcano, Southern Kermadec Arc: A paradox in the K-Depth relationship. *Canadian Mineralogist*, Vol. 35, 275-290, (1997).

Goldstein, H., R. and Reynolds, T. J.: Systematics of Fluid Inclusions in Diagenetic Minerals. *SEPM Short Course* 31, 198 p., (1994).

Graham, U. M., Bluth, G. J. And Ohmoto, H.: Sulfide-sulfate chimneys on the East Pacific Rise, 11° and 13° N latitudes. Part I: Mineralogy and Paragenesis. *Canadian Mineralogist*, 26, 487-504, (1988).

Hanor, S. J.: Synthesis of barite, celestite and barium-strontium sulphate solid solution crystals. *Geochim. Cosmochim. Acta*. V 37-12, 2685-2687, (1973).

Heinrich, E. W.: Microscopic Identification of Minerals, McGraw Hill, New York. p., 126-129, (1965).

Hoefs, J.:Stable Isotope Geochemistry. Springer-Verlag, pp. 1-196, (1997).

Holger, W. J.: Microbial processes at deep Hydrothermal Vents. In: Rona et al, (1983) Hydrothermal Processes at Sea Floor Spreading Centers. *NATO Conference Series*, IV. New York, (1983).

Lewis D. W. and McConchie D.: Analytical Sedimentology. Chapman and Hall, New York., (1994).

Mineral Powder Diffraction File Data Book, Sets 1-42: International Center for Diffraction Date, Pennsylvania, U.S.A., (1993).

Ohmoto, H. and Lasaga, A. C.: Kinetics of reactions between aqueous sulphates and sulphides in hydrothermal systems. *Geochim. Cosmochim. Acta* 46, 1727-1745, (1982).

Roedder, E.: Fluid Inclusions. Reviews in Mineralogy. *Mineralogical Society of America*. V. 12, p. 494-495, (1984).

Rona, P. A.: Hydrothermal mineralization at oceanic ridges. *Canadian Mineralogist*, 26, 431-465, (1988).

Rona, P. A. and Scott, S. D.: A special issue on sea-floor hydrothermal mineralization: new perspectives, Preface: *Econ. Geol*, 88, 1933-1976, (1993).

Scott, S. D.: Submarine hydrothermal systems and deposits. In: Barnes, H. L., ed., *Geochemistry of Hydrothermal Ore Deposits*; 3rd edition. New York: John Willey & Sons Ltd., 797-875, (1997).

Scott, S. D.: Deep Ocean Mining. *Geoscience Canada*, V. 28-2, p. 87-96, (2001).

Smith, I. E. M., Worthington, T. J., Price, R. C. and Gamble, J. A.: Primitive Magmas in Arc-Type Volcanic Associations: Examples from Southwest Pacific. *Canadian Mineralogist.* Vol. 35, 257-273, (1997).

Stoffers, P., Wright, I. C., de Ronde, C., Hannington, M., Villinger, H. and Herzig, P.: EOS, Little-studied Arc-Backarc System in the Spotlight. Transactions, *American Geophysical Union* 80,32, 353-359, (1999a).

Stoffers, P., Hannington, M., Wright, I. C., Herzig, P. I. and de Ronde C.: Elemental mercury at submarine hydrothermal vents in the Bay of Plenty, Taupo Volcanic Zone, New Zealand. *Geology*, vol. 27, No. 10. p 931-934, (1999b).

Thompson, A. J. B. and Thompson, J. F.H.: Atlas of alteration. *Geol. Ass. of Canada* 26-31, (1996).

Urabe, T., and Kusakabe, M.: Barite silica chimneys from the Sumisu Rift, Izu-Bonin Arc: possible analog to hematitic chert associated with Kuroko deposits. *Earth Planet. Sci. Lett*. 100, 283-290, (1990).

Wright, I. C., Stoffers, P., Hannington, M., de Ronde C. E. J., Herzig, P., Smith, I. E. M. and Browne, P. R. L.: Towed camera investigations of shallow-intermediate water-depth submarine stratovolcanoes of the southern Kermadec arc, New Zealand. *Mar. Geol.* 185, 207-218, (2002).